

Predicting Flow Function of Bulk Solids  
Based on Particle Size and Moisture Content

by

Anindya Deb

A Thesis Presented in Partial Fulfillment  
of the Requirements for the Degree  
Master of Science

Approved April 2021 by the  
Graduate Supervisory Committee:

Heather Emady, Chair  
Hamidreza Marvi  
Yang Jiao

ARIZONA STATE UNIVERSITY

May 2021

## ABSTRACT

The way a granular material is transported and handled plays a huge part in the quality of final product and the overall efficiency of the manufacturing process. Currently, there is a gap in the understanding of the basic relationship between the fundamental variables of granular materials such as moisture content, particle shape and size. This can lead to flowability issues like arching and ratholing, which can lead to unexpected downtimes in the whole manufacturing process and considerable wastage of time, energy, and resources. This study specifically focuses on the development of a model based on the surface mean diameter and the moisture content to predict the flow metric flow function coefficient (FFC) to describe the nature of flow of the material. The investigation involved three parts. The first entailed the characterization of the test materials with respect to their physical properties - density, size, and shape distributions. In the second, flowability tests were conducted with the FT4 Powder Rheometer. Shear cell tests were utilized to calculate each test specimen's flow function parameters. Finally, the physical properties were correlated with the results from the flowability tests to develop a reliable model to predict the nature of flow of the test specimens. The model displayed an average error of -6.5%. Predicted values showed great correlation with values obtained from further shear cell tests on the FT4 Rheometer. Additionally, particle shape factors and other flowability descriptors like Carr Index and Hausner Ratio were also evaluated for the sample materials. All size ranges displayed a decreasing trend in the values of Carr Index, Hausner Ratio, and FFC with increasing moisture percentages except the 5-11 micron glass beads, which showed an increasing trend in FFC. The results from this investigation could be helpful in designing equipment for powder handling and avoiding potential flowability issues.

This work is dedicated to

*Maa and Baba*

## ACKNOWLEDGMENTS

I would like to express my gratitude for the incredible guidance and encouragement that I have received from my advisor, Dr. Heather Emady. Her invaluable insights have been paramount in shaping this piece of research. During my time at The Particulate Process and Product Design Lab, Dr. Emady has been instrumental in my growth as a researcher, imbuing in me scientific rigor and temperament. She has always been a steady source of support, be it in academic, or personal goals. For all this, I would always be grateful to her. I would also like to thank my research supervisor, and doctoral candidate, Spandana Vajrala for teaching me the ropes of bulk solids research and always being around for all the mundane questions that might have popped up in my head and making me feel at home at the research group right from Day 1.

Additionally, I would like to thank my committee members, Dr. Hamidreza Marvi and Dr. Yang Jiao for their suggestions and feedback through the course of this research.

For financial support, I would like to thank Dr. Emady; Master's Opportunity for Research in Engineering (MORE) award from ASU; Graduate Research Support Program from Graduate and Professional Student Association (GPSA) and The Graduate College, ASU

## TABLE OF CONTENTS

	Page
LIST OF TABLES .....	v
LIST OF FIGURES .....	vi
CHAPTER	
1 INTRODUCTION .....	1
1.1 Bulk Solids .....	1
1.2 Flowability .....	2
1.3 Quantifying Flowability .....	2
2 METHODOLOGY .....	5
2.1 Materials .....	5
2.2 Particle Characterization .....	5
2.3 Bulk Powder Characterization .....	7
2.4 Data Analysis .....	13
3 RESULTS AND DISCUSSION .....	19
3.1 Compressibility Measurements .....	19
3.2 Shear Cell Measurements .....	20
4 CONCLUSIONS .....	25
REFERENCES .....	26

## LIST OF TABLES

Table		Page
1.1.	Materials Personality to Describe Nature of Bulk Solids .....	2
1.2.	Comparison of Carr Index, Haunser Ratio, and FFC values .....	4
2.1.	Shape Factors and their Definitions .....	6
3.1	Density Based Flowability Descriptors : Carr Index, Hausner Ratio .....	19
3.2	Shear Cell Test Results and Equations of Fitted Curves .....	20

## LIST OF FIGURES

Figure	Page
2.1. Images of Particles Displaying Pendular, Funicular, and Capillary States .....	9
2.2. Shear Cell Test Vessel, Split to Remove Excess Material .....	11
2.3. Normal and Shear Stresses in a Complete Shear Cell Test .....	12
2.4. Derivation of FFC .....	13
2.5. Fitted Curve for 5-11 micron particle size range.....	14
2.6. Fitted Curve for 25-50 micron particle size range.....	14
2.7. Fitted Curve for 70-100 micron particle size range.....	15
2.8. Fitted Curve for 120-180 micron particle size range.....	15
2.9. Fitted Curve for 180-250 micron particle size range.....	16
2.10. Fitted Curve for 250-350 micron particle size range.....	16
2.11. Linear Regression for Coefficient of Particle Size .....	18
3.1. Comparison of Torque Values of Fine and Coarse Beads During Testing .....	22
3.2. Correlation Between Experimentally Obtained and Predicted FFC Values .....	24

# CHAPTER 1

## INTRODUCTION

### 1.1 Bulk Solids

The process of designing equipment that can handle bulk solids reliably is a particularly challenging task. Bulk solids consist of essentially numerous particles or granules of different sizes and shapes that together constitute the bulk. There does not exist a limit to their size, but must constitute separate particles and does not include muds, pastes, and slurries (Reece, 1989). The characteristic properties of such a material are dependent on a variety of factors, but major contributions are from the size, shape, surface texture, density, and moisture content of the particles. As such, the metrics required to be able to predict the flow of the bulk solid may not be apparent immediately. Something as simple as just the density of the bulk solid is dependent on the shape, size, and packing of the particles.

The nature of the bulk solid is an important consideration while designing material handling and storage equipment. Examples of problems caused in equipment due to insufficient attention paid to these properties are a plenty (e.g., blockage of pneumatic conveying, blockage of feeders, and uncontrollable flushing from storage hoppers. (Muzzio et al., 2002)

The properties of a bulk solid can be described in two possible ways:

1. By describing the characteristic properties of its constituent particles – size, shape, density, friability, density, and surface texture.
2. By describing the characteristics of the material in its whole bulk form – degree of compaction, moisture content, and flow properties due to interparticle properties



## 1.2 Flowability

Bulk solid flowability is defined as the ease with which a granular material is flowing under specific conditions (Bodhmaghe, 2006). This behavior of the bulk solid can be described in numerous ways. One of the earliest classifications of bulk solid classified under different personalities (Reece, 1989). Depending on their nature, they were – Neurotic, Sadistic, Masochistic, and Schizophrenic – these are listed in Table 1.1.

**Table 1.1** Materials personality to describe the nature of bulk solids (Reece, 1989).

<b>Material Personality</b>	<b>Description</b>
'Neurotic' materials	<ul style="list-style-type: none"><li>• Poor flowability</li><li>• Sticky or tacky</li><li>• Move awkwardly</li></ul>
'Sadistic' materials	<ul style="list-style-type: none"><li>• Corrosive</li><li>• Explosive</li><li>• Attack their surroundings</li></ul>
'Masochistic' materials	<ul style="list-style-type: none"><li>• Friable</li><li>• Degradable</li><li>• Suffer from their surroundings</li></ul>
'Schizophrenic' materials	<ul style="list-style-type: none"><li>• Hygroscopic</li><li>• Change their behavior pattern</li></ul>

## 1.3 Quantifying Flowability

While subjective descriptions based on 'personality' are helpful in describing the behavior of a bulk solid to some extent, they are not of much practical use and are insufficient on their own. There is a need for numerical descriptors that give a more concrete idea about the nature of the bulk solid. There are several methods to evaluate the relative flowability of bulk solids. The simplest is to measure the Angle of Repose (AoR) of the material, which

consists of two kinds –static and dynamic (Beakawi Al-Hashemi & Baghabra Al-Amoudi, 2018). The static angle of repose is the steepest angle made by the material when it is dropped in the form of a pile without it avalanching/collapsing, while the dynamic angle of repose is the angle made by the inclined surface of the material with the horizontal when it is rotated in a drum. A powder with a steeper angle is said to have a lower ‘flowability’ than a powder with shallower angle. Angle of repose has been used in combination with powder densities as well to come up with other metrics to describe flow. Wouter and Geldart (Wouters & Geldart, 1996) quantified the effects of consolidation on powder flows by using the ratio of the static angle of repose to the aerated bulk density. Dury et al. also worked towards using different methodologies to measure static and dynamic angles of repose to evaluate flowability of different mixtures of free-flowing and cohesive material, and developed a relation between the angle and composition, from which they attained theoretical angles of repose for cohesive materials (Dury et al., 1998).

Descriptors based on the compressibility of the bulk solid are also popularly used to quantify flowability. The Hausner ratio (Beakawi Al-Hashemi & Baghabra Al-Amoudi, 2018) is the ratio between the tapped density of a material and its bulk density (Thalberg et al., 2004), while the Carr Index is the ratio of the difference between the bulk and tapped density to the tapped density, times 100. The Carr Index (Bodhmage, 2006) assigns a score to the bulk solid between 0 and 100, with 0 being the worst possible flowability and 100 being the best. The parameter that was chosen for this investigation is called the *Flow Function Coefficient*, or FFC. It is the ratio of the consolidation stress to the unconfined yield strength, or cohesive strength, of a bulk solid. It is a dimensionless solid that is used to describe the nature of flow of the bulk solid numerically. FFC has positive non-zero values, with increasing FFC values indicating increasing flowability in bulk solids. **Table**

1.2 shows the different classifications of the Carr Index, the Hausner Ratio, and the FFC with their flowability descriptions alongside them.

**Table 1.2** Carr Index, Hausner Ratio, and FFC values to quantitatively describe the nature of bulk materials.

<b>Carr Index</b>	<b>Hausner Ratio</b>	<b>Flow Function Coefficient (FFC)</b>	<b>Flowability Description</b>
<10	1.00 – 1.11	$10 < \text{FFC}$	Excellent
11-15	1.12 – 1.18	$4 < \text{FFC} < 10$	Good
16-20	1.19 – 1.25	$2 < \text{FFC} < 4$	Fair
21-25	1.26 – 1.34		Passable
26-31	1.35 – 1.45	$1 < \text{FFC} < 2$	Poor
32-37	1.46 – 1.59	$\text{FFC} < 1$	Very Poor
>38	>1.60		Very, Very Poor

FFC is a relatively easily available quantifier that is widely used in the industry to describe or rank the flowability of bulk solids. This was also one of the reasons it was chosen as the subject of this investigation. The goal was to develop a model that would be able reliably predict the FFC for a bulk solid with a particular particle size and moisture content, without having to perform experiments every time. Resulting in savings in resources and energy.

## CHAPTER 2

### METHODOLOGY

#### 2.1 Materials

Silica glass beads of varying sizes were obtained from Potters Industries, LLC. These were rated by the manufacturer in the size ranges of 5-11 microns, 25-50 microns, 70-100 microns, 120-180 microns, and 250-350 microns. These sizes were chosen to represent a wide spectrum of powder flowability – from very cohesive powders to comparatively free-flowing powders.

The characterizations were made based on the particle size and size distribution, particle shape, and density. Various techniques like image analysis and tapped density measurements were utilized.

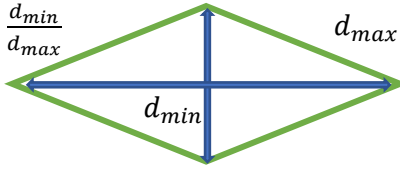
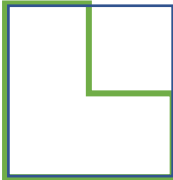
#### 2.2 Particle Characterization

The size distribution of the particles was measured using the Morphologi G3 (Malvern Instruments Ltd., Malvern, UK). This instrument measures the size, shape, and quantity of particles. The powder sample is loaded into the dispersion unit and is then dispersed onto the observation plate of the instrument. The instrument then proceeds to capture multiple images of the dispersed powder sample. The on-board software then processes these images to calculate particle mean sizes, particle size distributions and various shape factors. The final reported data includes the following size metrics: 10<sup>th</sup> percentile mean diameter, 50<sup>th</sup> percentile mean diameter, 90<sup>th</sup> percentile mean diameter, surface mean diameter –  $d_{3,2}$ , and volume mean diameter –  $d_{4,3}$ . For the present study, the surface mean diameter -  $d_{3,2}$  was taken as the principal size parameter for all calculations (Kowalczyk & Drzymala, 2016). It is the surface area mean size of the particle populations,

and for the study of flowability effects (that are governed by surface phenomena like surface roughness, adhesion, and cohesion), this parameter was deemed the most appropriate for this application.

Along with the particle size quantities mentioned above, the Morphologi G3 provides us with the following shape factors: aspect ratio, elongation, convexity, circularity, and circle equivalent diameter. Definitions and geometric representations of these shape factors are presented in **Table 2.1**.

**Table 2.1** Shape factors and their definitions.

Shape Factor	Definition	Equation
Aspect Ratio	<ul style="list-style-type: none"> <li>- The ratio of the smallest diameter to the largest diameter orthogonal to it.</li> <li>- Ranges between 0-1</li> </ul>	$AR = \frac{d_{min}}{d_{max}}$ 
Elongation	<ul style="list-style-type: none"> <li>- A measure of the degree of elongation of a particle.</li> <li>- Ranges between 0-1</li> </ul>	$E = 1 - AR$
Convexity	<ul style="list-style-type: none"> <li>- A measure of the surface roughness of a particle.</li> <li>- Ranges from 0-1, with 1 being a very smooth object, and 0 an extremely irregular one.</li> </ul>	$C_x = \frac{\text{Perimeter of convex hull}}{\text{Perimeter of Shape}}$ 
Circularity	<ul style="list-style-type: none"> <li>- A measure of how close to a circle the shape under consideration is.</li> <li>- Ranges from 0-1, with 1 being a perfect circle.</li> </ul>	$C = \sqrt{\frac{4\pi(\text{Area})}{\text{Perimeter}^2}}$
Circle Equivalent Diameter	<ul style="list-style-type: none"> <li>- Also known as are-equivalent diameter, is defined as the diameter of a circle with the</li> </ul>	$x_a = \sqrt{\frac{4(\text{area of particle})}{\pi}}$

	same area as that of the shape under consideration.	
--	-----------------------------------------------------	--

### 2.3 Bulk Powder Characterization

Bulk and tapped density measurement experiments were performed on the dry bulk solid specimens adhering to US Pharmacopeia standard: <616> *Bulk Density and Tapped Density of Powders* (USPC, 2014). The dry sample was gently poured into a 250 ml graduated cylinder and was carefully levelled, avoiding compacting the powder. The uncompacted powder level is then recorded ( $V_0$ ) to the nearest graduated unit. The mass ( $m$ ) of the sample is recorded and the bulk density is calculated by taking the ratio of the mass to the uncompacted powder volume ( $V_0$ ),  $\frac{m}{V_0}$ . Then cylinder is then secured onto the Sotax TD1 and then 10, 500, 1250 taps are performed on the sample and the corresponding volumes  $V_{10}$ ,  $V_{500}$ , and  $V_{1250}$  were recorded. The difference between  $V_{500}$  and  $V_{1250}$  is evaluated. If found to be less than or equal to 2%, then  $V_{1250}$  was taken as the tapped volume,  $V_F$ . If not, the sample was tapped further in increments of 1250 taps until a difference in volume of 2% was observed. The tapped density was then calculated as  $\frac{m}{V_F}$ . The tapped density was measured thrice, and the average of the values was used for the calculation of the Carr Index and the Hausner Ratio.

Test specimens for the FT4 powder rheometer were prepared by mixing the different powders with distilled water to create moisture levels of 0.5%, 1%, 5%, 10%, and 15% by weight. An upper limit of 15% moisture content was chosen because it was observed from previous studies that above this threshold, the bulk solid transforms into a different flow regime altogether (Kleppe, 2019), and it was not deemed practical to try to describe that

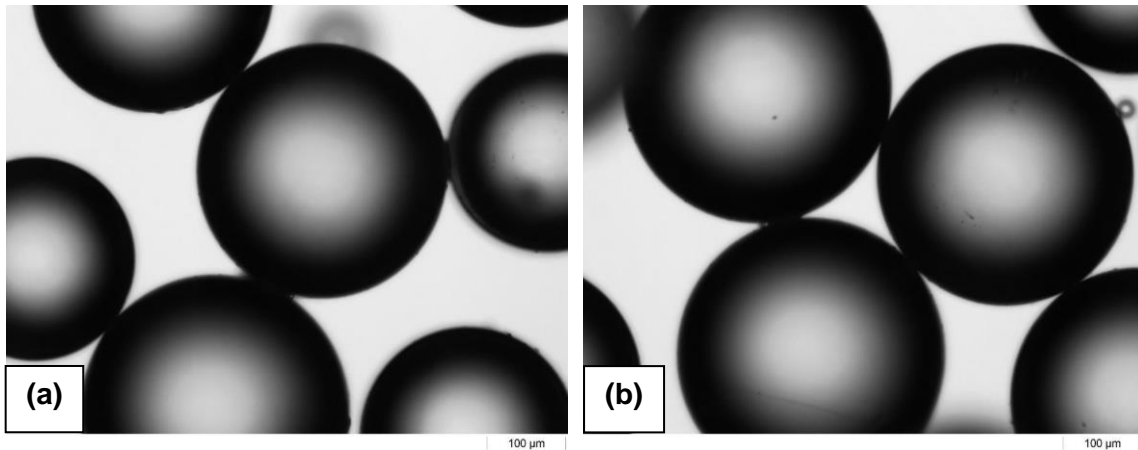
regime with the same empirical model. Similarly, dry powders were also excluded from the study, as it was observed that they displayed behavior akin to a different flow regime.

Distilled water was added to the material to make up the required moisture percentage for each test run, calculated by weight. The granular material and water were then kneaded together by hand until the mixture was homogeneous. It was ensured that the wet specimens were prepared just before the test so that consolidation over time and evaporation did not affect the test.

**Figs. 2.1 (a) – (e)** are images of glass beads of  $d_{3,2} = 309.9 \mu\text{m}$  at different moisture percentages taken with the Malvern Morphologi G3. The glass beads can be described to be existing in three distinct states (Chen et al., 2020), depending on their intensity of liquid saturation. The glass beads at 0.5%, 1%, and 5% moisture content, **Fig. 2.1 (a) – (c)**, displayed short and narrow bridges forming between the beads. This state is called the *pendular state*. The beads in these cases are held together by the bonding forces developed due to the liquid bridges. As the liquid content increases, the mixture changes to a *funicular state*, as can be seen in **Fig. 2.1 (d)**, which shows the glass beads at 10% moisture content. Along with the liquid bridges increasing in volume considerably, the voids in between the beads also start filling up. The beads are acted upon by the bonding force of the liquid bridges along with the pressure deficiencies introduced due to the surface tension of the water. On further increasing the moisture percentage to 15% (**Fig. 2.1 (e)**), the mixture transitioned into the *capillary state*, where the capillary forces come into full effect and hold the bulk solid together.

These wet specimens were then poured into the vessel of the FT4 Rheometer for subsequent shear cell tests. The FT4 is a powder flow tester for the measurement of powder properties and powder behavior.

The FT4 utilizes 'Test Programs' to perform each experiment which are run automatically by the equipment, other than the change of the various attachments for different parts of the test. The test program is a sequence of steps that the instrument takes during a test, which can also be altered to suit a particular use case. A custom test program was run for the wet test specimens adhering to ASTM D7891-15 standards (American Society for Testing Material, 2015), except that the initial conditioning sequence was omitted as it would trigger a 'blade height' error as the cohesive material would stick to the outer edges of the vessel and lead the system to believe that the blade was still immersed in the bulk material.





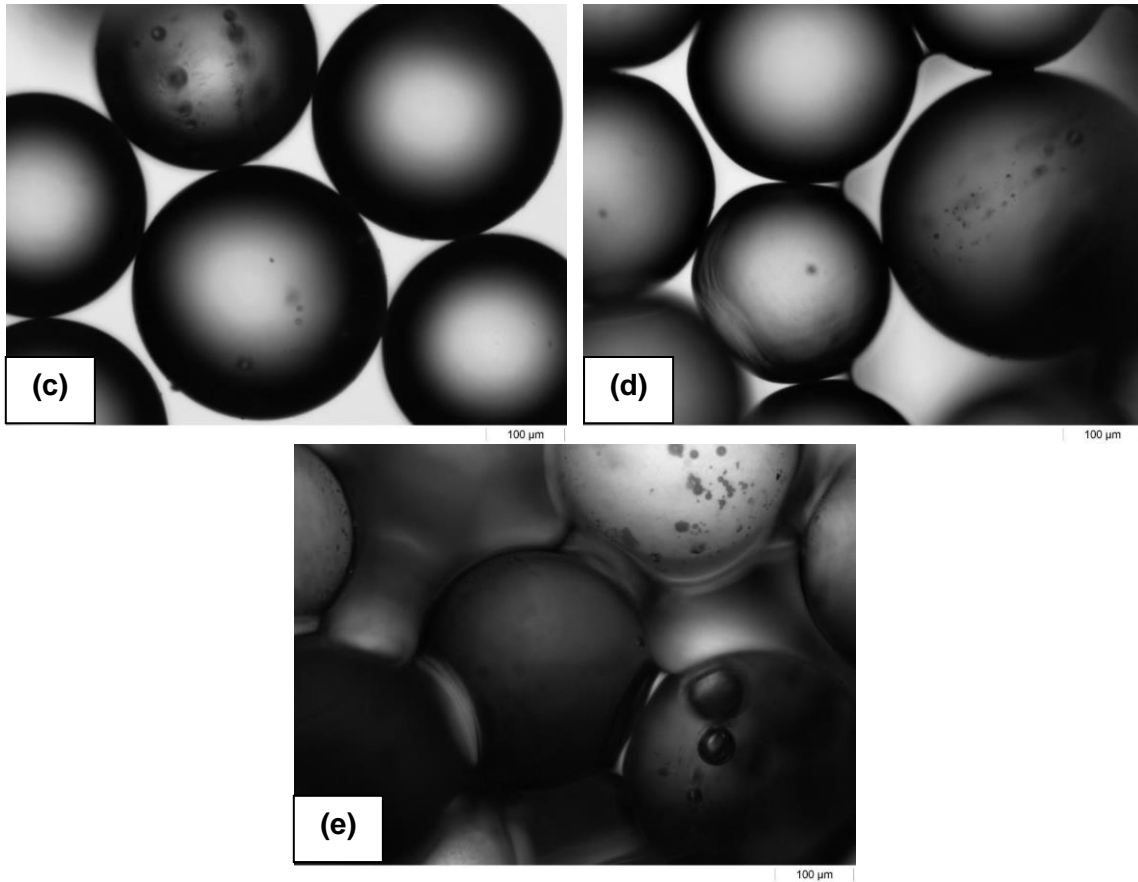


**Fig. 2.1** (a) and (b) show 309.90  $\mu\text{m}$  particles at 0.5% and 1% moisture contents, respectively. Liquid bridges can be seen forming between the glass beads, the bonding energy from these bridges binds the particles together. This is called the *pendular state*. (c) shows the particles at 5% moisture content, still in the *pendular state*. The increased liquid bridge volumes result in increased bonding strength and particles being packed closer together. **Fig. 2.1** (d) shows particle at 10% moisture, in the *funicular state*. The liquid start filling up the inter-particle voids and the surface tension forces of the liquid start coming into play. Finally, (e) shows the particles at 15% moisture content, displaying *capillary state*. Due to the increased liquid volume, the inter-particle bonding is affected by the capillary pressure of the liquid.

The sequence of steps that were performed during a test are as follows:

1. The piston was used to compress the test material to a consolidating stress of 9 kPa, following which the vessel was split to remove excess powder by means of a levelling mechanism where the upper half of the vessel splits to expose a flat cross-section of the consolidated material. The shear cell test was performed on this cross section in the steps that followed.

2. The vented piston was then swapped with the shear cell. Before the actual shear stress testing began, a series of pre-shear sequences were performed. The consolidating stress was re-established with the shear cell and the material was pre-sheared until a steady state was reached. This process was repeated until two consecutive pre-shears were found to be within 97% of each other in value.
3. The shear stress testing then began with an initial normal stress of 9 kPa. Shear stress was applied to the test specimen until the point of incipient flow (shear test point) was reached.
4. This cycle of shearing until incipient flow was repeated for normal stresses of 7 kPa, 6 kPa, 5 kPa, 4 kPa, and 3 kPa, as shown in **Fig. 2.3**.



**Fig. 2.2** The vessel used for the shear cell test on the FT4. The splitting mechanism is used to get rid of the excess material, resulting in a flat surface for the experiment.

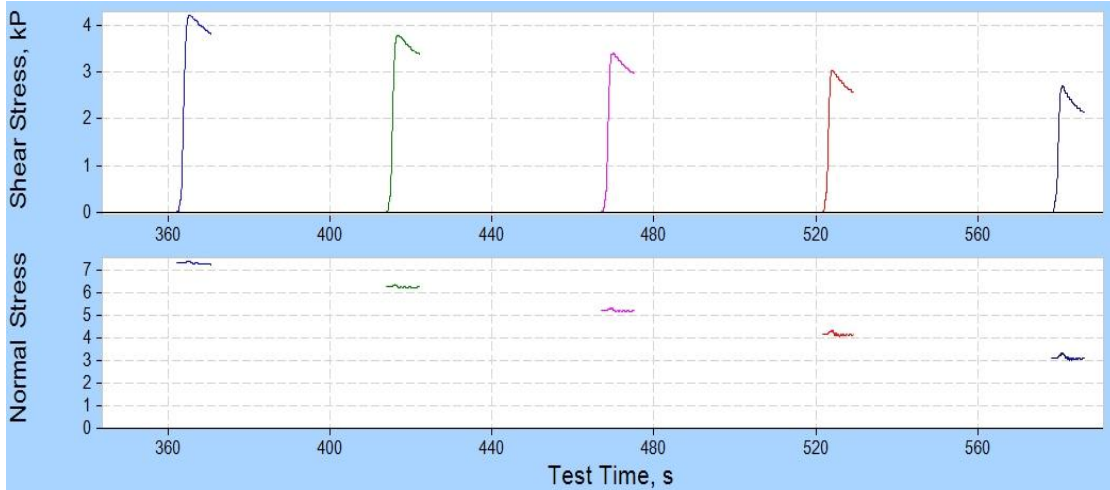


**Fig. 2.3** Successive shearing operations done in a single shear cell test experiment. The peak in the shear stress plots represents the point of incipient flow (shear test point) corresponding to each normal stress value.

The shear test points were plotted against their respective applied normal stress. A linear regression line was drawn through these data points to meet the y-axis. This line is known as the 'yield locus'. A Mohr's stress circle was drawn with its center on the x-axis, and tangential to the yield locus as shown in **Fig. 2.4**. The non-zero intercept of this circle gives us the unconfined yield strength,  $f_c$ , of the sample under consideration. A second Mohr's circle is drawn passing through the pre-shear point and tangential to the yield locus. This gives us two intercepts, the larger of which gives us the major principal stress,  $\sigma_1$ . The ratio of the major principal stress to the unconfined yield strength gives us the flow function coefficient (*FFC*) for each test specimen:

$$FFC = \frac{\sigma_1}{f_c} \quad (\text{Eq. 2.1})$$

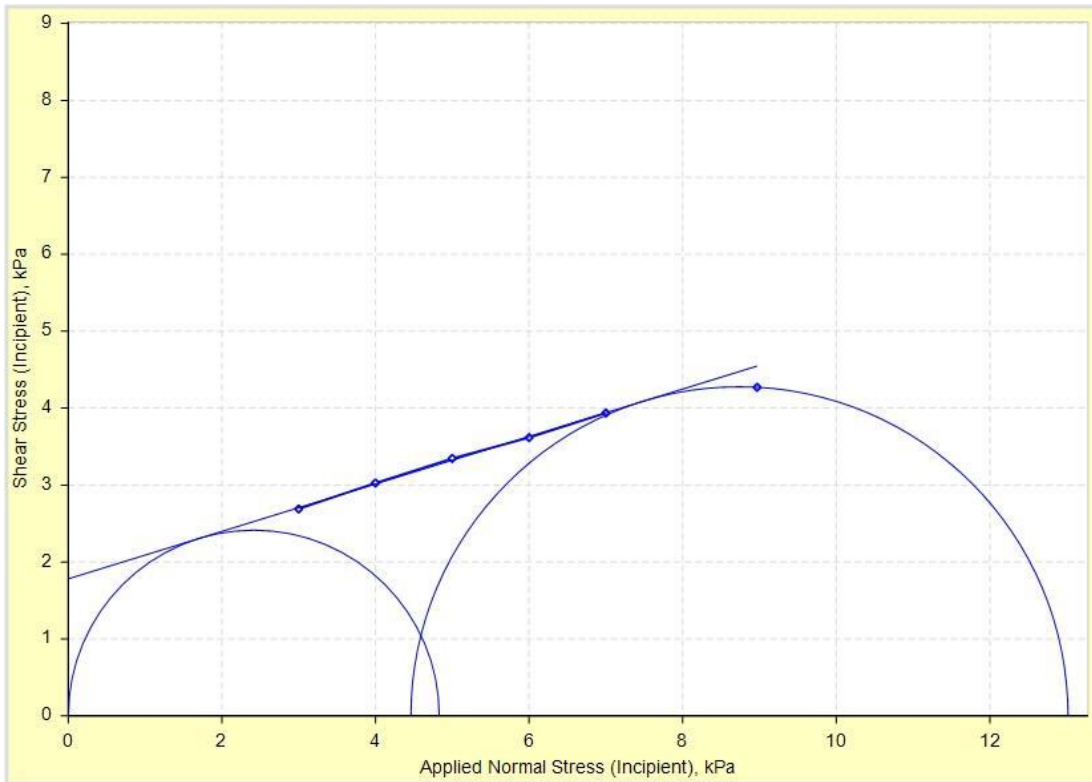


**Fig. 2.4** The construction of yield locus and the Mohr's circles. The values obtained from the intercepts of the circles are used to calculate the flow function coefficient.

## 2.4 Data Analysis

The average FFC values obtained were plotted against the moisture percentages for each size range. A data analysis and visualization software, CurveExpert Pro, was then used to find a curve that best fit these. The goodness of fit was evaluated by taking the  $R^2$ -value as the metric (see **Figs. 2.5–2.10**). It was observed that the data points were most accurately represented by equations of the *power-root* type.

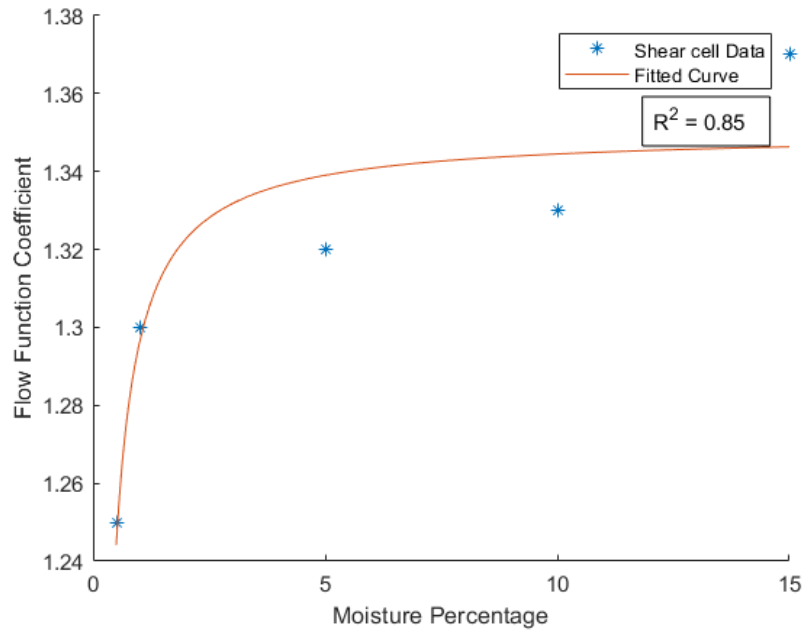


**Fig. 2.5** Fitted curve for the 5-11 microns particle size range.

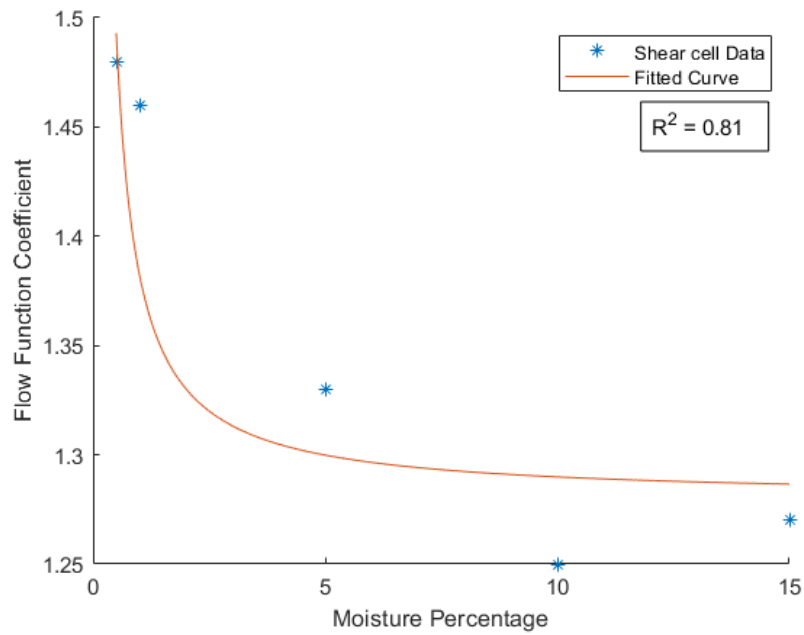


**Fig. 2.6** Fitted curve for the 25-50 microns particle size range.

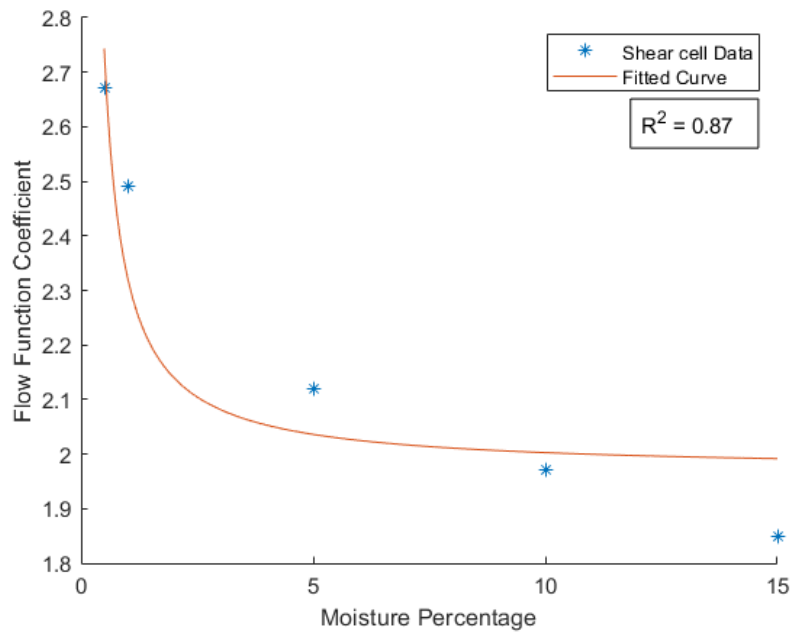


**Fig. 2.7** Fitted curve for the 70-100 microns particle size range.

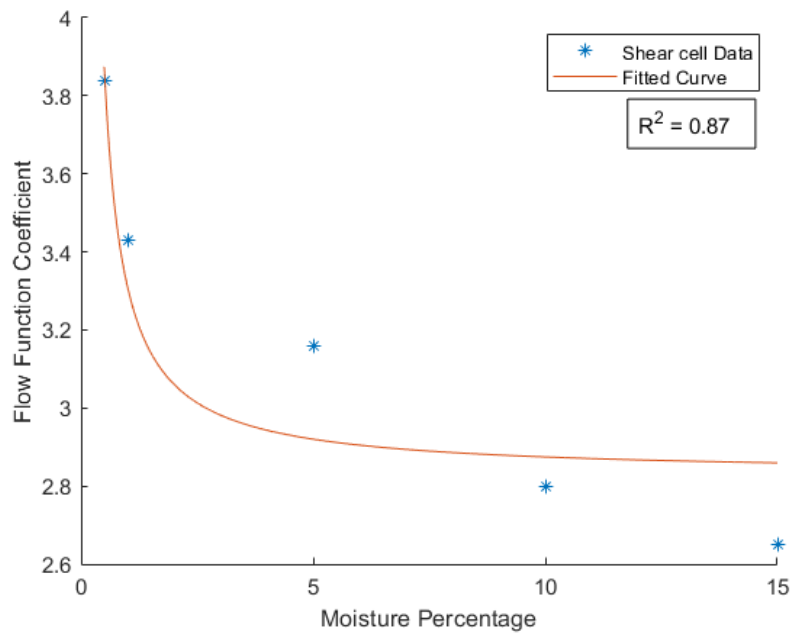


**Fig. 2.8** Fitted curve for the 120-180 microns particle size range.

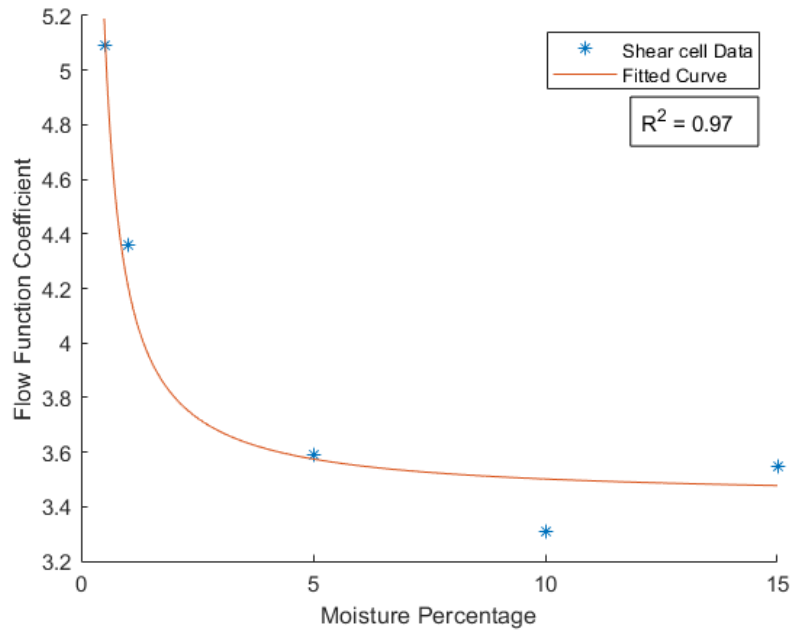


**Fig 2.9** Fitted curve for the 180-250 microns particle size range.

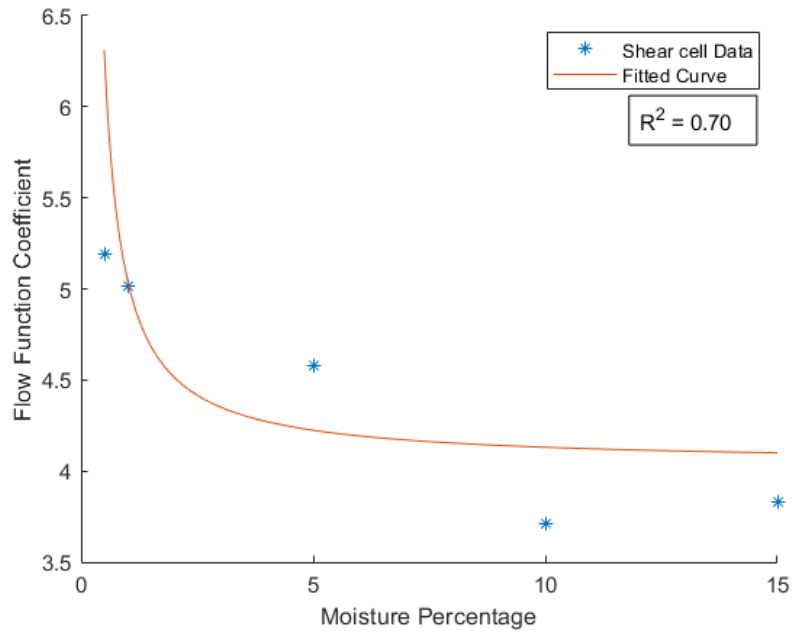


**Fig. 2.10** Fitted curve for the 250-350 microns particle size range.

The fitted curves thus obtained were of the following form:

$$FFC = (Coefficient\ of\ Particle\ Size)(Constant)^{\frac{1}{(Moisture\ Percentage)}} \quad (\text{Eq. 2.2})$$

The 'constant' term in the set of equations was observed to lie between 0.96 and 1.25. Values between these two limits were iteratively examined for best fit, and it was found that a value of 1.15 gave the most accurate values of FFC for the different combinations of particle size and moisture percentages used in the study.

In **Eq.2.2**, it was found that the first term varied significantly as the particle size was changed from test specimen to test specimen. This term was decided to be called the 'coefficient of particle size'. To obtain its relationship with the particle size, this coefficient from each equation was plotted against the surface area mean diameters, respectively. A linear regression line was developed to fit the data, as shown in **Fig. 2.11**. The fit obtained displayed a correlation coefficient value of 0.94, showing very good agreement with the data. The equation of the linear regression obtained from the plot in **Fig. 2.11**. is given as below,

$$\textit{Coefficient of particle size} = 1.28 + 0.1D_{3,2} \quad \textbf{(Eq. 2.3)}$$

Here,  $D_{3,2}$  is the surface area mean diameter of the particles.

This equation was then used to incorporate the effect of varying surface area mean diameters of the particles into the equation being developed.



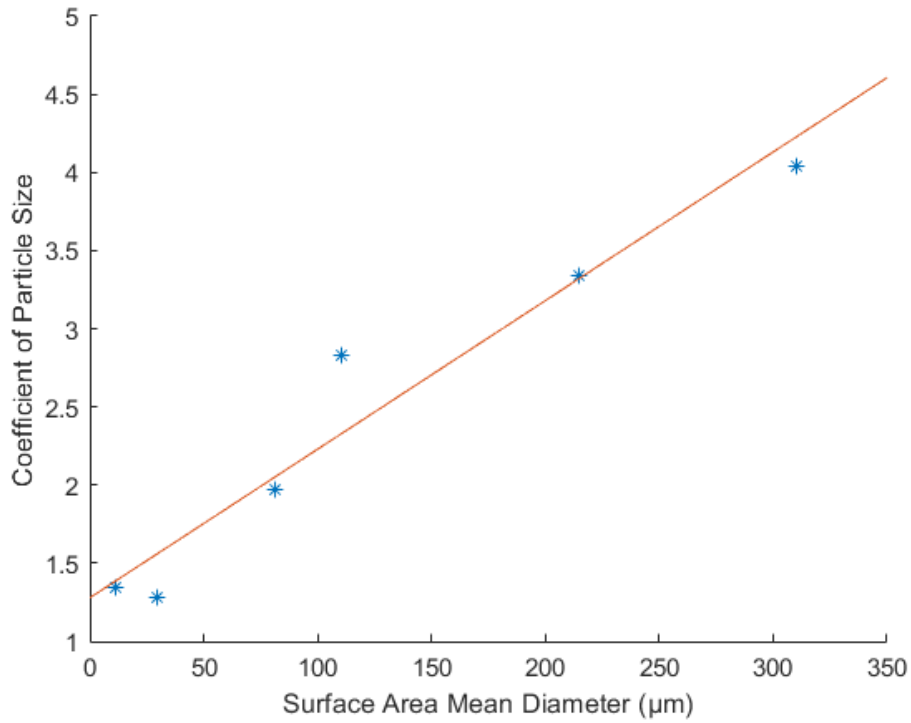


**Fig. 2.11** Coefficient of particle size plotted against the surface area mean diameters. A linear regression line is used to fit the data to develop a relationship between the two factors. The goodness of fit was evaluated by  $R^2$  value that was found to be 0.94.

## CHAPTER 3

### RESULTS AND DISCUSSION

#### 3.1 Compressibility Measurements

The results from the tapped density measurements, averaged over 3 experimental runs, done on dry silica beads, are shown in **Table 3.1**. Calculated values of Carr Index and Hausner Ratio are also presented. This provides an idea of the compressibility of the initial material used for the study.

**Table 3.1** Density-based flowability descriptors of the materials used in the study.

Size range ( $\mu\text{m}$ )	Tapped Density (g/ml) $\pm$ Std. Dev.	Initial Density (g/ml) $\pm$ Std. Dev	Carr Index	Hausner Ratio	Flowability Description
5-11	1.44 $\pm$ 0.05	0.87 $\pm$ 0.04	40	1.67	No Flow
25-50	1.53 $\pm$ 0.06	1.31 $\pm$ 0.06	14.3	1.17	Good
70-100	1.57 $\pm$ 0.07	1.42 $\pm$ 0.07	9.5	1.11	Excellent
120-180	1.57 $\pm$ 0.05	1.47 $\pm$ 0.05	6.5	1.07	Excellent
180-250	1.56 $\pm$ 0.07	1.48 $\pm$ 0.06	5	1.05	Excellent
250-350	1.57 $\pm$ 0.07	1.49 $\pm$ 0.07	5	1.05	Excellent

As can be seen from **Table 3.1**, the glass beads with particles in the size range of 5-11  $\mu\text{m}$  show the highest values of Carr Index and Hausner Ratio, indicating very high compressibility. On the other end of the spectrum, the materials in the 250-350  $\mu\text{m}$  size range have the lowest value of Carr Index and Hausner Ratio, indicating the lowest compressibility. These particles are also the freest flowing, as low values of Carr Index and Hausner Ratio correspond to better flowability. From the values in Table 3.1, it can be said that all bulk materials in the study with particle size greater than 70 microns have excellent flowability, the materials can also be listed as: 250-350  $\mu\text{m}$  > 180-250  $\mu\text{m}$  > 120-180  $\mu\text{m}$  > 70-100  $\mu\text{m}$  > 25-50  $\mu\text{m}$  > 5-11  $\mu\text{m}$  in the decreasing order of their ease of flow.

### 3.2 Shear Cell Measurements

The average of the FFC values for each combination of particle size and moisture content combinations from 3 runs were obtained. These FFC values were then plotted against the respective moisture percentages and the curve was fitted through these data points. The FFC values for each particle size range and the respective equation of the fitted curve are presented in **Table 3.2 (a) & (b)**. Tables (a) and (b) represented the particles size ranges that were used in the study and the ones that were excluded, respectively.

**Table 3.2 (a).** Results from the shear cell tests of the bulk solids that were used in the study, averaged over 3 runs for each particle size range and moisture content combination. The standard deviation of the average values of FFC is also shown.

Particle Size	Moisture %	Avg. FFC value ± Std. Dev.	Equation of Fitted Curve
5-11 µm D(3,2) = 11.4 µm	0.5	1.25 ± 0.01	FFC= 1.35* (0.96 <sup>(1/x)</sup> )
	1	1.3 ± 0.03	
	5	1.32 ± 0.05	
	10	1.33 ± 0.08	
	15	1.37 ± 0.10	
25-50 µm D(3,2) = 29.7 µm	0.5	1.48 ± 0.06	FFC = 1.28*(1.08 <sup>(1/x)</sup> )
	1	1.46 ± 0.01	
	5	1.33 ± 0.00	
	10	1.25 ± 0.00	
	15	1.27 ± 0.01	
70-100 µm D(3,2) = 81.5 µm	0.5	2.67 ± 0.03	FFC = 1.97*(1.18 <sup>(1/x)</sup> )
	1	2.49 ± 0.03	
	5	2.12 ± 0.08	
	10	1.97 ± 0.03	
	15	1.85 ± 0.02	
120-180 µm D(3,2) = 110.0 µm	0.5	3.84 ± 0.18	FFC = 2.83*(1.17 <sup>(1/x)</sup> )
	1	3.43 ± 0.09	
	5	3.16 ± 0.03	
	10	2.8 ± 0.05	
	15	2.65 ± 0.08	
180-250 µm D(3,2) = 215. µm	0.5	5.09 ± 0.42	FFC = 3.43*(1.23 <sup>(1/x)</sup> )
	1	4.36 ± 0.20	
	5	3.59 ± 0.04	
	10	3.31 ± 0.05	
	15	3.55 ± 0.14	

250-350 $\mu\text{m}$ $D(3,2) = 310. \mu\text{m}$	0.5	$5.19 \pm 0.28$	$\text{FFC} = 4.04 \cdot (1.25^{1/x})$
	1	$5.02 \pm 0.94$	
	5	$4.58 \pm 0.19$	
	10	$3.71 \pm 0.08$	
	15	$3.83 \pm 0.52$	

**Table 3.2 (b).** Results from the shear cell test of bulk solids that were excluded from the study after initial testing, averaged over 3 runs for each particle size range and moisture content combination. The standard deviation of the average values of FFC is also shown.

Particle Size	Moisture %	Avg. FFC value	Standard Deviation	Equation of Fitted Curve
430-600 $\mu\text{m}$	0.5	$8.68 \pm 2.06$		$\text{FF7}_F = (5.32)(1.322)^{1/x}$
	1	$8.74 \pm 4.90$		
	5	$5.98 \pm 1.78$		
	10	$4.12 \pm 0.70$		
	15	$5.28 \pm 3.89$		
600-850 $\mu\text{m}$	0.5	$7.45 \pm 2.26$		$\text{FF8}_F = (15.4)(1.121)^{1/x}$
	1	$9.67 \pm 8.95$		
	5	$8.4 \pm 8.09$		
	10	$1 \pm 1.53$		
	15	$7.55 \pm 7.59$		

The particles in the size range of 430-600 microns and 600-850 microns were excluded from the study after initial testing, as the standard deviation of the average values of FFC obtained from these size ranges were too high across all moisture percentages. **Table 3.2 (b)** shows the standard deviations of the averaged FFC values for the particle sizes that were excluded from the study. It is clear from the values that these two size ranges were outliers when compared to the other particles. The outliers were further investigated by evaluating the torque v/s time plots of the larger particles, as shown in **Fig. 3.1**. It was observed that there was a sharp drop in the torque value, caused due to the shifting of the whole powder column instead of the formation of a shear zone. This could be attributed to the physical constraints of the size of the shear cell, because of which a particle size of

about 350 microns was the upper limit for the FT4 Powder Rheometer. Above this upper size limit, the shear stress readings from the cell were found to be unreliable.

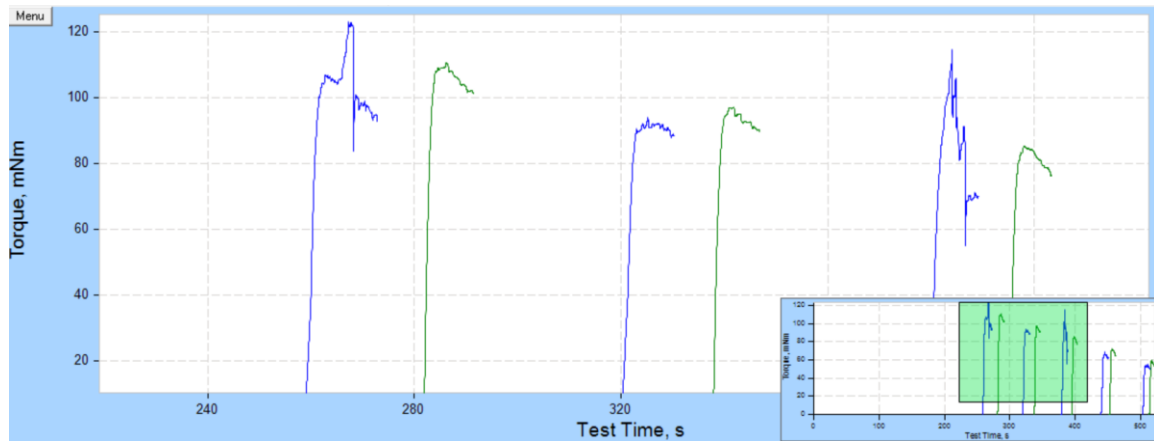


**Fig. 3.1** Torque values for 250-355 (green) and 430-600 (blue) micron glass beads with 0.5% moisture. The 430 – 600 micron particles with peaks demonstrate slippage in material.

Considering the remaining particle size ranges, we can see that the FFC value consistently decreases in all cases as the moisture percentage increases, except in the case of the 5-11 microns size range. This can be explained by the fact that in the case of very fine particles, the interparticle interaction is dominated by Van der Waals forces (Louati et al., 2017) and thus the corresponding curve (**Fig. 2.5**) for the fine powder starts with very low values of FFC – 1.25 and 1.3, which indicate a very cohesive flow of the material. Gradually, as the moisture percentage increases, the formation of tiny liquid bridges dissipates this effect, and the moisture starts acting as a lubricant, thus improving the flowability relative to the initial conditions.

For the larger size ranges, the Van der Waals forces are not as strong, and the particles are relatively free flowing. The addition of liquid to these particles leads to the formation of liquid bridges between the glass beads and this introduces bonding forces between the particles. As the liquid percentage increases and the interparticle voids start being

occupied by the liquid, surface tension forces and capillary pressure also come into play and make the bulk solid much more cohesive, thus negatively impacting the flowability. indicated by the decreasing FFC values.

The main goal of this study was to develop a model that could take into account the varying particle sizes and the moisture percentage in a bulk solid and then predict the flow function coefficient for the same. The effects of the varying particle size was incorporated in the final model by substituting the function acquired in **Eq. 2.3.** into **Eq. 2.2.** The final equation obtained is as follows,

$$FFC = (1.28 + 0.1D_{3,2})(1.15^{\frac{1}{moisture\ percentage}}) \quad (\text{Eq. 3.1})$$

where FFC is the flow function coefficient and  $D_{3,2}$  is the surface area mean diameter in microns.

**Eq. 3.1** was then used to make predictions for the FFC of different particle size-moisture content combinations. These predictions were then compared to experimentally obtained FFC values from shear cell tests performed on the FT4 Rheometer. The values predicted by the model were plotted against the values experimentally obtained from the shear cell tests, as shown in **Fig3.2.**

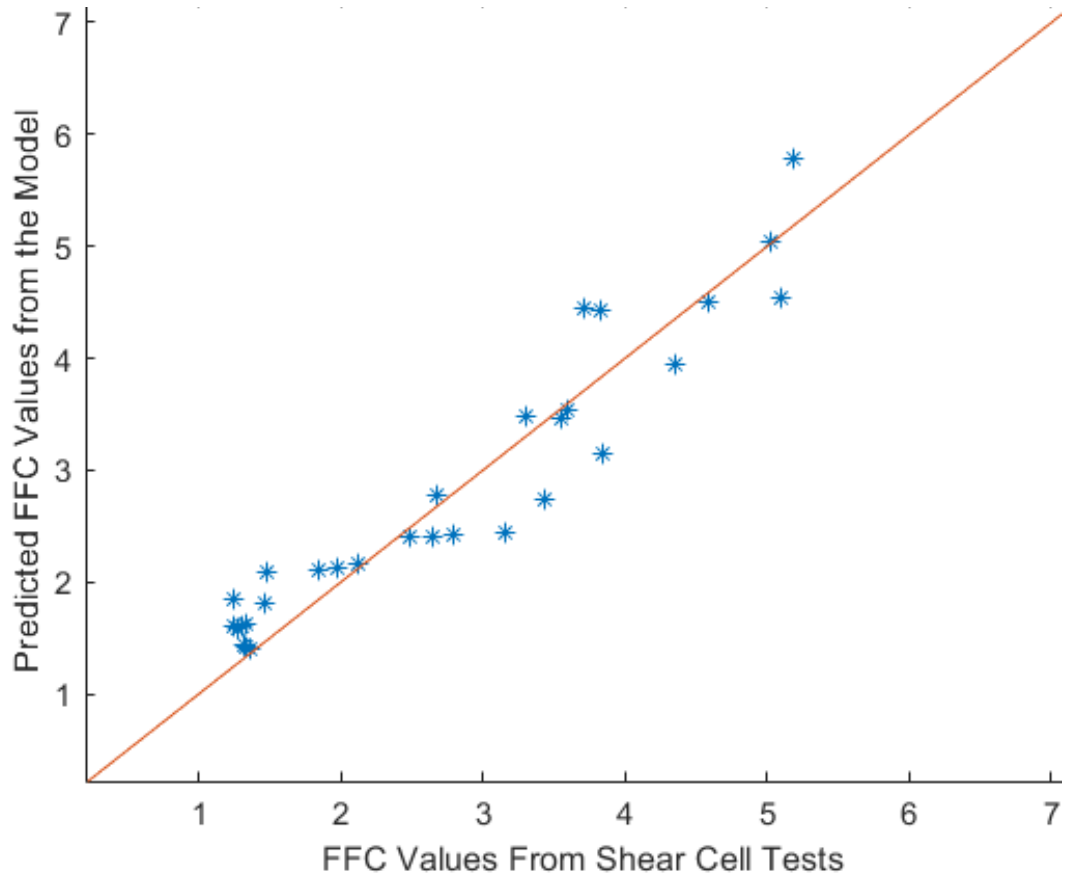


**Fig. 3.2** Correlation between the experimentally obtained values of the FFC and those predicted by the empirically developed model.

As can be seen from **Fig. 3.2**, the predicted and the experimental values are very closely bunched together along the  $y=x$  line, showing very good agreement, with a correlation coefficient of 0.91.

## CHAPTER 4

### CONCLUSIONS

The particle and bulk properties of silica beads of various sizes were characterized. Shear cell tests were performed on these particles under varying moisture content conditions. The results from these tests were then used to develop an equation to predict the flow function coefficient (FFC) of bulk materials based on particle size and moisture content. The model showed an average error of only -6.5% across the particle size ranges and moisture percentages tested. The model can reliably be used for bulk solids with particle sizes less than 350 microns and a non-zero moisture content less than 15%.

The predictions from the model could be used in the industrial setting as a tool to assess the flowability of a moist bulk solid or can be used to estimate the particle size or amount of liquid to be added to the blend for favorable flowability. Also, the model could be used to provide estimates for FFC values without having to perform tedious tests repeatedly, saving time and resources. Values obtained can be used to estimate the nature of flow of different pharmaceutical blends based on the surface area mean diameter of the particles.

An important area of future work would be to investigate the incorporation of a shape factor into the model. This would significantly improve the understanding of the bulk solid, as it has already been established that particle shape, along with particle size, plays a major role in affecting the flowability of a bulk solid. Another avenue that could be explored would be to include the whole particle size distribution in the model, leading to much more comprehensive and accurate predictions of the FFC.



## REFERENCES

- American Society for Testing Material. (2015). Standard test method for shear testing of powders using the freeman technology FT4 powder rheometer shear cell. *Astm D7891-15*, 1–11. <https://doi.org/10.1520/D7891-15.1.5>
- Beakawi Al-Hashemi, H. M., & Baghabra Al-Amoudi, O. S. (2018). A review on the angle of repose of granular materials. *Powder Technology*, 330, 397–417. <https://doi.org/10.1016/j.powtec.2018.02.003>
- Bodhmaghe, A. (2006). Correlation between physical properties and flowability indicators for fine powders. *University of Saskatchewan, July*, 1–122. <http://www.collectionscanada.gc.ca/obj/s4/f2/dsk3/SSU/TC-SSU-07032006115722.pdf>
- Chen, J., Williams, K., Chen, W., Shen, J., & Ye, F. (2020). A review of moisture migration in bulk material. *Particulate Science and Technology*, 38(2), 247–260. <https://doi.org/10.1080/02726351.2018.1504152>
- Dury, C. M., Ristow, G. H., Moss, J. L., & Nakagawa, M. (1998). Boundary effects on the angle of repose in rotating cylinders. *Physical Review E - Statistical Physics, Plasmas, Fluids, and Related Interdisciplinary Topics*, 57(4), 4491–4497. <https://doi.org/10.1103/PhysRevE.57.4491>
- Kleppe, C. (2019). Shear Stress Properties of Granular Materials by Cameron Kleppe. *Arizona State University*, 1(1).
- Kowalczyk, P. B., & Drzymala, J. (2016). Physical meaning of the Sauter mean diameter of spherical particulate matter. *Particulate Science and Technology*, 34(6), 645–647. <https://doi.org/10.1080/02726351.2015.1099582>
- Louati, H., Oulahna, D., & de Ryck, A. (2017). Effect of the particle size and the liquid content on the shear behaviour of wet granular material. *Powder Technology*, 315, 398–409. <https://doi.org/10.1016/j.powtec.2017.04.030>
- Muzzio, F. J., Shinbrot, T., & Glasser, B. J. (2002). Powder technology in the pharmaceutical industry: The need to catch up fast. *Powder Technology*, 124(1–2), 1–7. [https://doi.org/10.1016/S0032-5910\(01\)00482-X](https://doi.org/10.1016/S0032-5910(01)00482-X)
- Woodcock C.R., Mason J.S. (1987) The nature of bulk solids. In: Bulk Solids Handling. Springer, Dordrecht. [https://doi.org/10.1007/978-94-009-2635-6\\_1](https://doi.org/10.1007/978-94-009-2635-6_1)
- Thalberg, K., Lindholm, D., & Axelsson, A. (2004). Comparison of different flowability tests for powders for inhalation. *Powder Technology*, 146(3), 206–213. <https://doi.org/10.1016/j.powtec.2004.08.003>
- USPC, U. S. P. C. (2014). Method II-Measurement in a Volumeter. *The United States Pharmacopeial Convention*, 06(2012), 2014–2016. [https://www.usp.org/sites/default/files/usp/document/harmonization/gen-chapter/bulk\\_density.pdf](https://www.usp.org/sites/default/files/usp/document/harmonization/gen-chapter/bulk_density.pdf)

Wouters, I. M. F., & Geldart, D. (1996). Characterising semi-cohesive powders using angle of repose. *Particle and Particle Systems Characterization*, 13(4), 254–259. <https://doi.org/10.1002/ppsc.19960130408>